

# Optimization of weir structure design and flow calculation method using nonlinear programming in water conservancy canal system

Jia Yu<sup>1,\*</sup>

<sup>1</sup> Department of Resources Exploration and Civil Engineering, The Engineering & Technical College of Chengdu University of Technology, Leshan, Sichuan, 614000, China

Corresponding authors: (e-mail: yaobaideyu2021@163.com).

**Abstract** Weir flow measurement is an important content for safety monitoring of hydraulic buildings, and it is of great significance to strengthen the seepage monitoring of hydraulic buildings to ensure the safety of hydraulic buildings and feedback design. Based on the basic principles of optimal design of engineering structures and the theory of structural reliability, this paper uses nonlinear planning to optimize the structural design and flow calculation method of water-measuring weir in water conservancy canal system, and analyzes the hydraulic characteristics of the optimized water-measuring weir through numerical simulation, which verifies the effectiveness of the proposed method. The simulation results show that the influence of the new trapezoidal water-measuring weir with different orifice heights on the outflow over the weir gradually decreases with the increase of the total head in front of the weir, and the fitted flow equations are concise, easy to use and highly generalized, with an average relative error of 2.55%. At the same time, the average relative error of the flow and water depth of the U-shaped channel triangular profile weir is 0.22% and 5.76%, respectively, and the flow measurement accuracy of the long-throat channel optimized by the method of this paper is also controlled within 6%, which is in line with the flow measurement requirements of the water measuring channel, which indicates that the simulation results have a certain degree of reliability, and can provide a reference basis for the optimization of the design of the engineering structure of the water measuring facilities.

**Index Terms** nonlinear programming optimization, reliability, numerical simulation, structural design of water measuring weir, flow calculation; hydraulic characteristics

## I. Introduction

With the increase in population and socio-economic development, the utilization and management of water resources are receiving more and more attention. At present, industrialization and urbanization have increased the pollution of water resources, resulting in water-quality water shortages. Human production and life construction, economic development, energy use of water resources to increase the demand for water resources, caused by resource-based water shortage. The construction of a large number of water conservancy projects, the destruction of the ecological environment of water resources, is more likely to lead to engineering water shortage, so the shortage of water resources has become a fundamental problem that hinders economic development [1]-[4]. Water conservancy canal system is an important infrastructure, and its safe operation is directly related to the interests of agricultural irrigation, urban water supply, ecological environment, etc., which provides support for water resources management [5]. The total amount of water resources in China is large, temporarily ranked sixth in the world, but the per capita water resources in China is about 2239.8 m<sup>3</sup>, only 1/4 of the world average. Due to the progress of science and technology as well as the increasing awareness of human beings for water resources protection, some years even show a small increase in the total amount of water resources, but in general, it still shows a decreasing trend [6]-[9].

In recent years, China's total agricultural water consumption has always accounted for more than 60% of the country's total water consumption, and farmers' weak awareness of water conservation, as well as the lack of water-saving technology, has led to a great waste of agricultural water resources, so it is necessary to control the water use of agricultural irrigation and improve the efficiency of irrigation water use to make the necessary management measures [10]-[12]. Water measurement in irrigation area is the basic work of agricultural irrigation water management, the rational allocation of irrigation water, irrigation water utilization coefficient measurement, and the implementation of per-party charging system cannot be separated from water measurement in irrigation area, but there are very few water measurement facilities to meet the requirements of inexpensive, high-precision, convenient measurement, and strong anti-interference ability [13]-[15]. Therefore, the study of water measurement facilities to

meet the requirements of water measurement in irrigation areas is particularly urgent and important for agricultural water measurement. In order to adapt to the requirements of the new period to improve the level of irrigation management in the irrigation area, and to promote the rational allocation and efficient utilization of water resources, the canal system should be set up with water measuring facilities. Water measuring weir is a kind of water conservancy engineering facilities based on fluid mechanics and measurement principles, which is used to calculate the size of water flow, and mainly consists of weir dam, flume and flow measurement equipment [16]. The existing water measurement weir in the irrigation area generally exists in the low accuracy of flow measurement, elevated channel water level, head loss is large, the construction of complex body size is large and other shortcomings, but also generally exists in the large flow measurement is accurate, the small flow measurement deviation is large, does not adapt to the irrigation area of the last level of the canal system measurement of the water requirements, to the irrigation area of the accurate measurement of the reasonable distribution of water has caused a certain impact [17], [18]. In order to improve the water utilization rate, save valuable water head, and improve the accuracy of water measurement, the construction of simple construction, economical and practical, accurate water measurement facilities is the main means of water use control in irrigation districts, which not only provides the main basis for water quantity control and water fee collection, but also has an important significance in promoting water conservation and improving irrigation methods [19], [20]. Therefore, in order to promote water management in irrigation areas, it is imperative to improve the water measuring weir.

This paper combines the principle of optimal design of engineering structures and the reliability theory, and uses NLP method to realize the optimization of the structural design and flow calculation method of the water measuring weir in the water conservancy canal system. In order to verify the feasibility of the proposed method, trapezoidal water measuring weir, triangular water measuring weir and long-throat trough water measuring weir are selected for optimization design, analyze the distribution of water level and flow rate under different working conditions and the relationship curve between water level and flow rate, and calculate the flow measurement accuracy of the optimized water measuring weir, so as to provide the data support for the optimization of the structural design of water measuring weir.

## II. NLP-based structural design and flow calculation method for water measuring weir

### II. A. Fundamentals of optimal design of engineering structures

#### II. A. 1) Constraints for optimal structural design

In optimization models, there are generally two types of constraints: constant constraints and constraint equations. Constant constraints, also known as boundary limit constraints, give the allowable range of values for the design variables. The expression form of constraint equations is based on the selected structural optimization design variables as the independent variables, and the physical quantities corresponding to the constraints that must be satisfied to ensure the safety, reliability and applicability of the structure as the dependent variables, and according to a certain physical-mechanical relationships established by the corresponding functional relationship. When these relationships are expressed in the form of explicit functions, they are called explicit constraints. While the structural relationship is expressed in the form of implicit function, it is called implicit constraints. Generally, the geometric constraints reflecting the geometric interrelationships can often be expressed as explicit constraints, while the stress constraints, deflection and other deformation constraints, stability constraints, main frequency constraints and other structural state constraints can often only be expressed as implicit constraints.

In engineering optimization problems, engineering structural optimization problems containing geometric constraints and morphological constraints can be divided into two categories: linear planning problems and nonlinear planning problems, where the objective function and the constraint function are linear functions, and the objective function and the constraint function of the latter, where at least one of the objective function and the constraint function is a nonlinear function.

#### II. A. 2) Mathematical model for optimal structural design

If an engineering structural problem has  $n$  design variables, the mathematical model for its structural optimization can be formulated as:

Find the design variables:

$$x = [x_1, x_2, \dots, x_n]^T \quad (x \in R^n) \quad (1)$$

Make its objective function:

$$f(x) = f(x_1, x_2, \dots, x_n) \rightarrow \text{Min(Or Max)} \quad (2)$$

while satisfying the constraints:

$$\begin{cases} g_j(x) = g_j(x_1, x_2, \dots, x_m) \geq 0 & (j = 1, 2, \dots, m) \\ h_e(X) = h_e(x_1, x_2, \dots, x_n) = 0 & (e = 1, 2, \dots, p < n) \end{cases} \quad (3)$$

Expressed in the general form, i.e:

$$\begin{cases} \min f(x) = f(x_1, x_2, \dots, x_n) & (x \in R^n) \\ s.t. g_j(x) \geq 0 & (j = 1, 2, \dots, m) \\ h_e(x) = 0 & (e = 1, 2, \dots, p < n) \end{cases} \quad (4)$$

where:  $m$  and  $n$  are the number of inequality constraints and equation constraints, respectively.

### II. A. 3) Optimization of design variables

The purpose of optimal design of engineering structures is to select a most reasonable solution from all possible solutions. In the process of optimal design of structures, some of those physical quantities involved in the calculations are in the form of variables called design variables. Other physical quantities will be in the form of constants, which are called parameters. A structural design solution may be described by a number of design variables. In a mathematical model, the design variables constitute the “domain” of all possible structural design solutions, provided that they satisfy the design specifications and certain regulatory requirements, and the number of design variables is called the dimension of the optimization problem.

### II. A. 4) Optimizing the design objective function

In structural design optimization, the criterion used to judge whether the design scheme is superior or inferior is the objective function, which characterizes one of the most important features or indexes of the designed structure, such as the self-weight of the components, the volume of materials, the volume of the structure, the cost of the project or the cost of the project, the structural bearing capacity, the bending stiffness, the self-oscillation characteristics, etc. The objective function is a function of design variables. The objective function is a function of design variables. The process of optimal design is to take the objective function as a control criterion to find out the design variable values corresponding to the maximum or minimum values of this function from many feasible design solutions, i.e. to select the optimal design solution. In the objective function, the number of design variables to determine its dimensionality, and the power of the design variables to determine its linear or nonlinear characteristics, when all variables are a power, the objective function is linear, otherwise it is nonlinear.

### II. B. Nonlinear Planning Optimization Methods (NLP)

Nonlinear constrained optimization is an important part of nonlinear optimization problems. The essence of this type of model for nonlinear optimization is to find the extreme value of a single-valued function on a finite-dimensional real space, which may be governed by equational constraints or by inequality constraints. The standard form of a nonlinear programming problem is as follows:

$$\begin{cases} \min f(x) \\ s.t. \begin{cases} g_i(x) \leq 0 & i = 1, \dots, p \\ h_j(x) = 0 & j = 1, \dots, q \end{cases} \end{cases} \quad (5)$$

where  $x = (x_1, x_2, \dots, x_n)^T$ ,  $f(x)$ ,  $g_i(x)$ , and  $h_j(x)$  are real-valued functions of  $x$ ,  $f(x)$  is the objective function,  $g_i(x)$  is the inequality constraints, and  $h_j(x)$  is the equality constraints, and it is called an NLP when at least one of the three is nonlinear [21].

For the NLP model, iterative methods can be used to find its optimal solution. The basic idea of the iterative method is that, starting from a selected initial point  $x^0 \in R^n$ , a column of points  $\{x^k\}$  is generated according to a particular iterative rule, such that when  $\{x^k\}$  is an exhaustive column of points, the last point thereof is an optimal solution of the NLP model. When  $\{x^k\}$  is an infinite point column, it has limit points and its limit point is an optimal solution of the NLP model.

Let  $x^k \in R$  be the  $k$ th round of iteration points of an iterative method, and  $x^{k+1} \in R^n$  be the  $k+1$ th round of iteration points, then the basic iterative format for solving the NLP model is:

$$x^{k+1} = x^k + t_k p^k \quad (6)$$

where  $t_k \in R^1$ ,  $p^k \in R^n$ ,  $\|p^k\| = 1$ , and  $p^k$  is the direction determined by the point  $x^k$  and the point  $x^{k+1}$ .

According to the basic iteration formula, the optimization process is obtained as follows:

Step1: Select the initial point  $x^0$  and make  $k = 0$ .

Step2: Construct the search direction, according to the constraints, so that the search direction is the feasible descent direction of  $f$  at  $x^k$  about  $K$ .

Step3: Find the next iteration point based on the iteration formula:

$$x^{k+1} = x^k + t_k p^k \quad (7)$$

Step4: Replace  $x^k$  with  $x^{k+1}$  and return to Step2.

Step5: Repeat the above steps until the optimal solution is obtained.

In this paper, the NLP optimization method is used for the structural optimization of the water measuring weir, which adopts the dynamic process associative solving strategy to completely discretize the differential-algebraic model equations and optimization problem through the finite element polynomial configuration method. The discretized model is characterized by more equation constraints, relatively low variable degrees of freedom and sparse structure. Therefore, in this paper, by discretizing the flow measurement process of the water measuring weir, the finite element polynomials are established by using the parameters of the shape, angle and size of the weir, and the cooperation relationship between the measuring devices of the weir is used as the constraints, which ultimately achieves the purpose of optimizing the design of the weir structure and the flow calculation. The specific flow of the nonlinear planning optimization method to optimize the structure of the water measuring weir is shown in Figure 1.

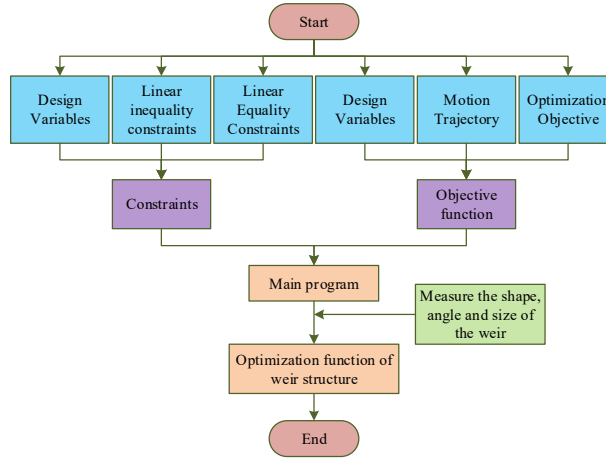


Figure 1: Flow chart of NLP method to optimize weir structure

## II. C. Reliability-based structural optimization design of water-measuring weir

Structural reliability, a probabilistic measure of structural reliability, is the probability that a structure will fulfill its intended function within a specified time and under specified conditions, also known as the probability of reliability [22]. In this section, a nonlinear programming optimization of the structural design of the gauging weir is carried out based on the theory of structural reliability.

### II. C. 1) Optimization of design issues

The conventional structural optimization problem is shown in equation (8):

$$\begin{cases} \min f(x) = f(x_1, x_2, \dots, x_n) & (x \in R^n) \\ s.t. g_j(x) \leq 0 & (j = 1, 2, \dots, m) \\ h_e(x) = 0 & (e = 1, 2, \dots, p < n) \end{cases} \quad (8)$$

where the constraint equations  $h_e(x) = 0$  and  $g_j(x) \geq 0$  are geometric and dispositional constraints. Among the temperament constraints, they are generally stress constraints, such as the maximum stress at the danger point does not exceed the code allowable value i.e.  $\sigma_{\max} - [\sigma] \leq 0$ , and displacement constraints, such as the mid-span deflection of the beam does not exceed a certain limiting value i.e.  $V_{\max} - [V] \leq 0$ , and so on.

Whereas, in reliability-based structural optimization problems, the constraint equations are given in terms of the failure probability or reliability index of the structure, e.g., when establishing the constraint equations in terms of the structural failure probability, the stress condition is expressed as follows: the probability of the maximum stress at the hazardous point,  $\sigma_{\max}$ , exceeding the normative allowable value,  $[\sigma]$ ,  $P_f$ , is not exceeded by the target failure probability,  $[P_f]$ , i.e:

$$P_f = P\{\sigma_{\max} \geq [\sigma]\} \leq [P_f] \quad (9)$$

When the constraint equation is established with the reliability index  $\beta$ , the above stress condition is expressed as follows: the maximum stress at the hazardous point  $\sigma_{\max}$  does not exceed the code tolerance value  $[\sigma]$  and the reliability index  $\beta$  is not less than the target reliability index  $[\beta]$ , viz:

$$\beta = \beta\{\sigma_{\max} \leq [\sigma]\} \geq [\beta] \quad (10)$$

In reliability analysis, stress conditions are generally replaced by load capacity conditions, such as flexural capacity of the member in the normal section, shear capacity in the diagonal section, and so on.

When the structural arrangement and the materials used are certain, the structural optimization problems based on reliability are of the following two types:

(1) The first type of optimization problem

That is, the optimization problem “to minimize the structural volume or cost under the constraints of structural target reliability or structural failure probability”, and its mathematical model is expressed as follows:

Find the design vector:

$$X = [x_1, x_2, \dots, x_n]^T \quad (11)$$

Make the objective function:

$$f(X) = f(x_1, x_2, \dots, x_n) \quad (12)$$

is minimum (or maximum) and satisfies the constraints:

$$g_j(X) = [\beta] - \beta_j(X) \leq 0 (j = 1, 2, \dots, m) \quad (13)$$

where:  $m$  denotes the number of temperament constraints.  $\beta_j(X)$  denotes the structural reliability metric for the  $j$  th constraint.  $[\beta]$  denotes the objective reliability index.

(2) The second type of optimization problem

It is to design the structure under the constraint that the “volume or cost” of the structure is a definite value, so that the reliability index of one or several functions in terms of load carrying capacity and usability can reach or exceed the target value stipulated in the specification, and its mathematical model can be expressed as follows:

Find the design vector:

$$X = [x_1, x_2, \dots, x_n]^T \quad (14)$$

Make structural reliability indicators:

$$\beta_j(X) \geq [\beta] (j = 1, 2, \dots, m) \quad (15)$$

and fulfill the conditions:

$$W_e(X) - W \leq 0 (e = 1, 2, \dots, p) \quad (16)$$

Where:  $m$  is the number of structural safety and reliability control indicators.  $P$  is the number of economic control indicators.

The second type of optimization problem has actually become a multi-objective optimization problem. In this paper, the structural optimization problem of water-measuring weir belongs to the first type of optimization problem.

### II. C. 2) Solution methods

There are two main types of solution paths to solve the structural optimization problem based on the reliability theory: the mathematical planning method and the optimization criterion method. The former is based on the function value and derivative value of the current design scheme, according to some rules, in the multidimensional design variable space, automatically generate a logical optimization process, and gradually carry out the search until the optimal solution is approximated, in which the function value and derivative value corresponding to each step of the new scheme are derived according to the structural analysis method. Its advantage is that it can solve a variety of different nature of the optimization problem, good generality, but its disadvantage is that the number of iterations increases with the number of variables. Optimization criterion method, on the other hand, is based on the physical or mechanical properties of the problem, the establishment of a certain optimization criterion, on the basis of which the corresponding iterative formula, or in accordance with the mathematical planning theory of the Kuhn-tucker conditions to establish the optimization iterative formula. The former is called the intuitive criterion method, and the latter is called the rational criterion method. The advantage of the criterion method is that the number of variables has little effect on the calculation volume, but the generalization is poor and the convergence is not guaranteed, which is suitable for the initial design stage of the structure.

### II. C. 3) Optimization steps for water measuring weir structure

In view of the above analysis, and taking into account the nature of the structural optimization problem of the water-measuring weir studied in this paper, this paper selects the composite shape method belonging to the mathematical planning class of methods for solving the problem, in which the calculation of structural reliability indexes is based on the method of checking points, and the steps of the structural optimization calculation of the water-measuring weir are shown in Fig. 2.

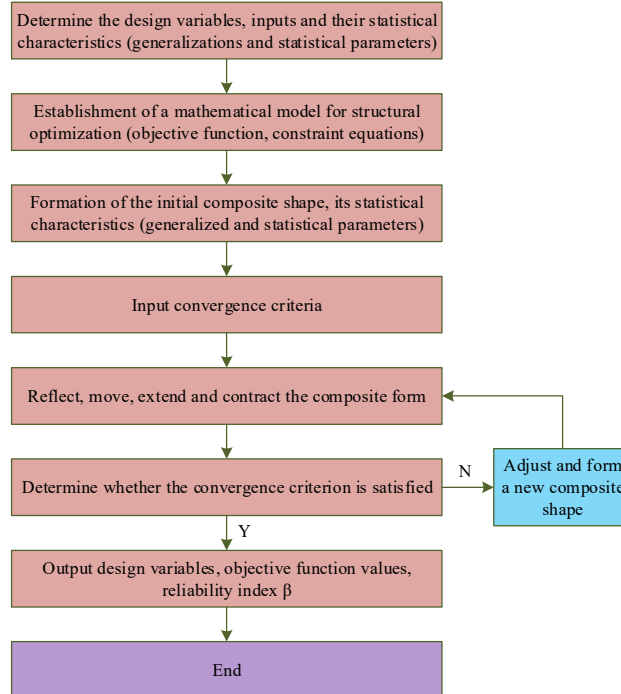


Figure 2: Flowchart of structural optimization calculation

## II. D. Measurement Principles and Design of Water Measuring Weirs

### II. D. 1) Weir flow measurement methods

#### (1) Principle of weir flow measurement



Weir flow is a water flow phenomenon in which the slow flow overflows through the top of the baffle after the baffle (weir) is set in the open channel. Due to the role of the baffle, the water level in front of the plate will rise, when the flow rate from the weir is equal to the flow rate of the channel, the water level in front of the weir and the flow rate over the weir has formed a stable relationship between the relationship is determined by the structure of the shape of the weir plate to block the water, through the measurement of this time the height of the water level, you can be based on the corresponding relationship between the flow rate. The higher the flow in the nullah, the higher the level will be, and the lower the flow, the lower the level will be.

The method of measuring the flow rate of the weir is suitable for the flow rate between 1-300L/s, and the measurement in this range has a high measuring accuracy. When the flow rate is between 1-70L/s, the triangular water measuring weir is used, and experiments have proved that the right-angle triangular weir is suitable for the flow rate of less than 30L/s. Trapezoidal weir is suitable for measuring flow between 10-300L/s. Rectangular weir is mostly used for measuring flow between 1-300L/s and 1-300L/s. The rectangular water measuring weir is mostly applied to the flow greater than 50L/s. When the flow range is large, the rectangular water measuring weir can be combined with the triangular water measuring weir to form a composite weir for measurement.

## (2) The choice of water measuring weir and its structural design

The main purpose of this paper is to optimize the structural design and calculation method of water measuring weir, and the main factors to be considered for the selection of water measuring weir include experimental conditions, the complexity of water measuring weir fabrication, the measuring range of weir flow, and the accuracy requirements. This paper mainly carries out design and measurement experiments on triangular water measuring weir, trapezoidal water measuring weir and wide top weir.

## II. D. 2) Flow calculation formulas

### (1) Formula for calculating the flow rate of triangular water measuring weir

Hydraulic modeling experiments used in the right-angle triangular water measurement weir flow calculation formula usually contains three independent factors, respectively, for the flow coefficient  $C$ , weir tank width  $B$  and weir head  $H$ , in the hydraulic modeling experiments in the textbook used in the calculation of the flow formula for:

$$Q = CBH^{5/2} \quad (17)$$

The flow coefficient  $C$  is not a fixed value, will be with the water level, the width of the tank and other changes and take a different value. Flow coefficient  $C$  value is calculated as:

$$C = 1.354 + \frac{0.004}{H} + \left( 0.14 + \frac{0.2}{\sqrt{P}} \right) \left( \frac{H}{B} - 0.09 \right)^2 \quad (18)$$

The applicable range of this formula is  $p = 0.01 \sim 0.75m$ ,  $B = 0.44 \sim 1.18m$ ,  $H = 0.07 \sim 0.25m$ .

In this paper, the formula for calculating the overflow capacity  $Q$  of the delta weir with respect to the relevant parameters is deduced using the method of magnitude analysis. The analysis shows that the overflow capacity of right-angled triangular water measuring weir is related to six factors, which are head over weir  $H$ , weir channel width  $B$ , weir height  $P$ , density  $\rho$ , gravitational acceleration  $g$ , viscosity coefficient  $\mu$ , etc., and then the overflow capacity  $Q$  can be expressed by the following functional equation:

$$Q = f(H, B, P, \rho, g, \mu) \quad (19)$$

For the basic physical quantities,  $H$ ,  $\rho$ , and  $g$  can be chosen, and then  $Q$  can be expressed by a functional equation consisting of other dimensionless parameters, which are calculated by using the method of magnitude analysis [23]:

$$Q = f\left(\frac{f}{H}, \frac{p}{H}, \frac{\mu}{H^{3/3} \rho g^{1/2}}\right) g^{1/2} H^{5/2} \quad (20)$$

Order:

$$C = f\left(\frac{f}{H}, \frac{p}{H}, \frac{\mu}{H^{3/3} \rho g^{1/2}}\right) g^{1/2} \quad (21)$$

Then there is:

$$Q = CH^{5/2} \quad (22)$$

In this paper, the corrected fitted empirical formula is used:

$$Q = 1.33H^{2.465} \quad (23)$$

## (2) Flow calculation formula of trapezoidal water measuring weir

Trapezoidal water measuring weir flow calculation formula and triangular water measuring weir flow calculation formula is similar, only the flow coefficient is different, and the index relationship with the formation of the water level is also different. The formula for calculating the flow over the weir is:

$$Q = 1.86Bh^{\frac{3}{2}} \quad (24)$$

where:  $Q$  indicates the flow rate over the weir ( $m^3/s$ ),  $B$  indicates the width of the weir mouth ( $m$ ),  $h$  indicates the depth of water over the weir ( $m$ ), and 1.86 is the flow coefficient.

The weir outlet form of various water measuring weir has two cases of free outflow and submerged outflow, and the experiment shows that when free outflow is used, the water measuring weir has higher accuracy in measuring the flow, so in the research of this paper, the water level and flow rate calculation method under the case of free outflow is adopted.

### (3) Iterative method for flow calculation

In hydraulics, taking into account the water mobility characteristics, often design iterative method to carry out the calculation of flow, in order to reduce the measurement error caused by water fluctuations. Take the standard triangular water measurement weir as an example to illustrate the process of flow calculation by iterative method:

1) List the values of head ( $h$ ), bottom width ( $B$ ), and weir height ( $p$ ).

2) Calculate the flow coefficient ( $C$ ) using equation (17).

3) Approximate it step by step:

Setp1: Substitute weir width  $B$ , water level height  $h_1$ , and flow coefficient  $C_0$  into flow calculation formula (17) to calculate the initial approximation of flow  $Q_1$ .

Setp2: Based on the value of  $Q_1$ , find the new water level information  $h_2$  on the standard water level-flow curve or in the water level-flow table.

Setp3: Substitute the value of  $h_2$ , as well as the weir width  $B$  and weir cantilever  $p$  into Equation (18) to calculate the new value of flow coefficient  $C_2$ .

Setp4: Substitute the values of  $C_2$ ,  $B$  and  $h_2$  into Eq. (17) again to calculate the second approximation of the flow rate  $Q_2$ .

4) Repeat the above steps until the error existing between the calculated flow rate and the flow rate obtained from the previous calculation is within the permissible limits.

## II. D. 3) Design of measuring devices

The water measuring weir designed in this paper is mainly for measurement and practice in the laboratory. For the measurement of water level and flow rate need a whole device composed of water supply tank, flowing water nullah, water measuring weir plate and so on, in order to carry out the experiment, the specific requirements are:

(1) The bottom and sides of the device are well sealed. If the water tank or water facilities leak, it will affect the water level, which will cause errors in the flow measurement results.

(2) The device needs to have a certain load-bearing capacity. Because in the measurement process, there will be more water flow in the channel, has a certain weight, need to channel and water supply tank has enough bearing capacity.

(3) Flow rate can be adjusted to facilitate the experiment. In the experimental process, it is necessary to monitor a variety of different flows within the measurement range, and it is necessary to adjust the flow size to control the height of the water level on the weir for measurement.

Based on the above requirements, the experimental device using 4mm transparent plexiglass plate as the material, in accordance with the optimized engineering design drawings spliced together, between each glass plate



using chloroform firmly bonded, in order to ensure the sealing of the use of silicone rubber filler after bonding. Considering that water has volatility in the flow, which affects the accurate measurement of water level, the device is perfected, that is, according to the principle of the connecting device, a small container is connected externally at the location of the water level measurement, so that it is connected to the channel, so that the measurement of the water level height in the channel is transformed into the measurement of the water level height in the outer container.

### III. Numerical simulation of water measuring weir and analysis of results

In this paper, the proposed structural design optimization method is applied to the structural optimization of trapezoidal weir, triangular weir and wide top weir, and the hydraulic characteristics of these new weirs are simulated numerically to verify the feasibility of the proposed method.

#### III. A. Hydraulic Characterization of New Trapezoidal Measuring Weir

##### III. A. 1) Depth and flow before weir

In this section, numerical simulation is used to simulate the total flow rate  $Q=17.34, 20.21, 23.46, 28.19, 32.43, 39.57$ , and  $43.12$  L/s for each of the improved weir and the four new trapezoidal water-measuring weirs with orifice heights  $z$  of 40, 50, 60, and 70 mm, and the difference of inlet and outlet flow rates of less than 1% is taken as a condition of convergence, and a monitoring section to monitor the outflow flow over the weir.

The measured and simulated weir head values are compared and analyzed as shown in Table 1. Where  $H$  denotes the total head measured at 0.7m upstream of the weir plate, and  $\delta$  denotes the relative error. The maximum relative error between the simulated value and the test value is 5.70%, and the average relative error  $\bar{\delta}$  is 2.55%, which indicates that the simulation of the new trapezoidal water measuring weir using Fluent software is an effective and reliable method.

Table 1: Comparison of test values with simulated values

z/mm	Q/(L·s <sup>-1</sup> )	H/m		$\delta\%$	z/mm	Q/(L·s <sup>-1</sup> )	H/m		$\delta\%$
		Test value	Simulated value				Test value	Simulated value	
40	17.34	0.1531	0.1575	-2.87	50	17.34	0.1524	0.1537	-0.85
	20.21	0.1857	0.1918	-3.28		20.21	0.1921	0.1845	3.96
	23.46	0.1947	0.1836	5.70		23.46	0.1734	0.1681	3.06
	28.19	0.2297	0.2336	-1.70		28.19	0.1936	0.2023	-4.49
	32.43	0.2113	0.2075	1.80		32.43	0.2015	0.2069	-2.68
	39.57	0.2513	0.2594	-3.22		39.57	0.2525	0.2397	5.07
	43.12	0.2478	0.2437	1.65		43.12	0.2409	0.2394	0.62
60	17.34	0.1526	0.1461	4.26	70	17.34	0.1445	0.1413	2.21
	20.21	0.1604	0.1649	-2.81		20.21	0.1506	0.1537	-2.06
	23.46	0.1808	0.1728	4.42		23.46	0.1604	0.1615	-0.69
	28.19	0.1906	0.1895	0.58		28.19	0.1792	0.1836	-2.46
	32.43	0.1935	0.1861	3.82		32.43	0.1917	0.1873	2.30
	39.57	0.2266	0.2245	0.93		39.57	0.2098	0.2114	-0.76
	43.12	0.2292	0.2336	-1.92		43.12	0.2283	0.2258	1.10

##### III. A. 2) Effect of orifice overflow on outflow over a weir

Related literature research shows that when the water flows through the hole weir structure water discharge building, there will be water stratification under the influence of the building, respectively, from the building on the top and bottom through, and there will be an internal role between the top and bottom through the flow, mutual influence.

The new weir structure compared to improve the weir at the bottom of the additional orifice, the structural difference will make the original improvement of the weir of the overflow law changes, this need for the new weir weir on the overflow law research. In this paper, the monitoring section on the weir is set in Fluent software, so as to obtain the overflow on the weir under different bottom hole heights and different flow conditions, and the monitoring value of the section on the weir is compared with the calculated value of the formula of the improved weir fitted in the relevant literature, as shown in Fig. 3. Where (a)~(d) denote the orifice height  $z$  of 40, 50, 60 and 70 mm, respectively.

The monitoring values of overflow over the weir with different orifice heights under different total heads before the weir are all slightly larger than the calculated values of the formula, which indicates that after the addition of the bottom orifice, the overflow over the weir is promoted by the orifice overflow. Through the analysis, it can be seen

that the overflow from the weir has a downward velocity component in the process of falling, and the weir flow in the downstream of the channel and the convergence of the orifice flow, the weir flow by the influence of the orifice flow changes in the flow rate of the weir flow, and the orifice flow of the weir flow into the flow rate is shown as a kind of promotional effect, which increases the flow rate of weir flow, so the flow rate is increased. Examining the characteristics of the difference between the monitoring value and the calculated value, it can be seen that the fluctuation range is from 0.54 to 2.01L/s, and the difference gradually decreases with the increase of the flow rate, which indicates that with the increase of the flow rate, the influence of the orifice overflow on the overflow on the weir is getting smaller and smaller.

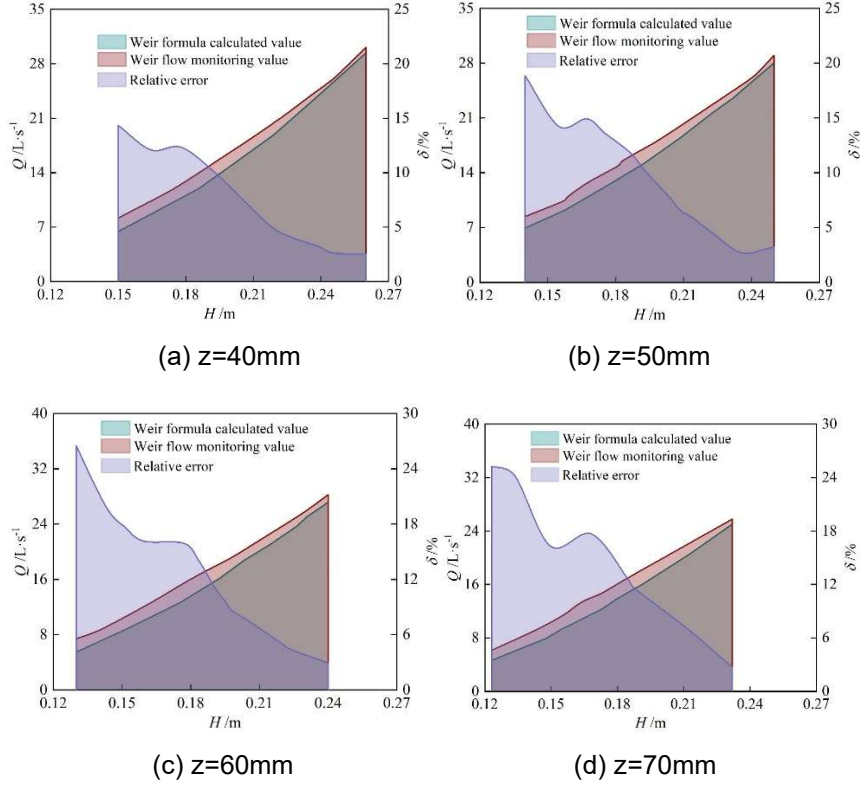


Figure 3: Comparison of weir flow monitoring value and formula calculation value

### III. A. 3) Combined flow coefficients

It is found that the integrated flow coefficient  $C$  is most significantly related to  $h/z$ ,  $H/z$ . From the new weir structure, it can be seen that the total head in front of the weir  $H = h + d + z$ , and when converted to  $H/z$ , it is found that it has more part of the size effect ( $d, z$ ) than  $h/z$ , which makes the correlation between the integrated flow coefficient  $C$  and  $H/z$  worse, so the paper analyzes the relationship between the integrated flow coefficient  $C$  and  $h/z$ .

The relationship between the integrated flow coefficient  $C$  and  $h/z$  is shown in Fig. 4. The integrated flow coefficient  $C$  of the new weir with different orifice heights increases with the increase of  $h/z$ . The fitting of different  $h/z$  with the calculated integrated flow coefficient shows that the complex correlation coefficient reaches 0.997. Based on the principle of simple, easy-to-use and generalizability of the formula, the relationship between the integrated flow coefficient  $m$  and  $h/z$  is obtained, and the flow measurement formula of the new type of weir with different orifice heights is calculated as shown in Eq. (25):

$$Q = \left[ 0.0964 \left( \frac{h}{z} \right)^2 + 0.875 \frac{h}{z} + 0.431 \right] \sqrt{2gbz^{1.5}} \quad (25)$$

The range of application is as follows:  $Q = [0.015, 0.046] \text{ m}^3/\text{s}$ ,  $b = 280 \text{ mm}$ ,  $z = [40, 70] \text{ mm}$ ,  $h = [0.03, 0.18] \text{ m}$ ,  $p = 120 \text{ mm}$ .

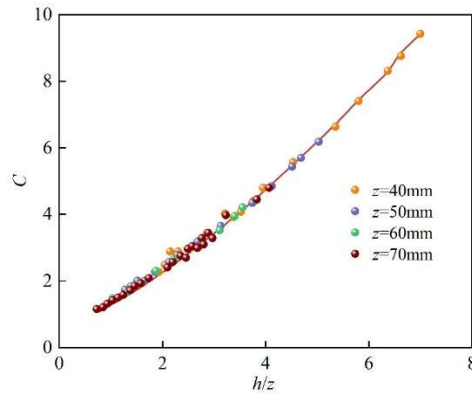


Figure 4: Relationship between comprehensive flow coefficient  $C$  and  $h/z$

Calculate the flow rate values at different weir front heads with different bottom hole heights and compare them with the measured values, and the comparison results are shown in Table 2.

From Table 2, it is learned that the maximum relative error of flow rate of equation (25) is 5.49%, and the average relative error is 2.58%, which meets the requirements of the national agricultural water measurement accuracy. As the formula (25) can be calculated for different orifice height of the new weir flow, eliminating the need to re-rate the integrated flow coefficient due to the different height of the orifice, the formula is more versatile. For the improved weir of  $b = 280\text{mm}$ , a rectangular orifice with a height of 60mm can be set at the bottom of the weir plate to form a new type of weir, at which time the maximum relative error of the calculated flow rate is 3.26%, and the maximum overcurrent flow rate expands by 480% compared with the standard type and 36% compared with the improved weir, with a high improvement in the scope of application, which can be applied in production practice.

Table 2: Comparison result between measured flow values and calculated flow values

$z/\text{mm}$	$h/\text{cm}$	$H/\text{m}$		$\delta/\%$
		Calculated value	Measured value	
40	6.89	19.52	20.24	3.56
	9.54	22.27	23.43	4.95
	11.27	27.63	28.32	2.44
	14.21	38.77	38.73	-0.10
	14.08	43.17	43.21	0.09
50	5.34	17.2	17.68	2.71
	7.95	23.06	23.55	2.08
	10.04	27.9	28.18	0.99
	13.54	39.6	38.85	-1.93
	14.79	43.56	43.21	-0.81
60	4.7	17.38	17.66	1.59
	5.7	20.7	20.39	-1.52
	7.99	28.04	28.15	0.39
	11.66	39.88	38.62	-3.26
	13.35	44.29	43.1	-2.76
70	4.87	18.47	17.62	-4.82
	6.12	24.72	23.52	-5.10
	7.67	28.83	28.01	-2.93
	9.35	33.84	32.52	-4.06
	12.96	45.55	43.18	-5.49

### III. B. Hydraulic characterization of U-shaped channel triangular profile weir

In this section, numerical simulations are carried out on the U-shaped channel triangular profile weir obtained by structural optimization of the triangular water measuring weir to analyze its hydraulic characteristics, to further verify the effectiveness of the optimization method of structural design and flow calculation in this paper.

### III. B. 1) Model validation

Select the effective water depth upstream, use the formula to calculate the corresponding flow rate, according to the flow rate to calculate the corresponding inlet velocity, the simulation of the water surface line, read the simulated depth of water, and the use of weir flow formula to calculate the simulated depth of water corresponding to the simulation of the flow rate, will be selected from the effective depth of water and simulation to get the simulation of the depth of water compared with the simulation of the design flow rate with the simulation of the flow of the simulated volume of comparison. In this paper, the effective water depth is selected as 0.40m, 0.37m, 0.35m, 0.34m, 0.32m, 0.29m, and the simulation results are shown in Table 3.

Table 3 shows that the average relative error and the maximum relative error of flow rate are 0.22% and 0.35% respectively, and the average simulation error and the maximum relative error of water depth are 5.76% and 8.57% respectively, and the simulated values of flow rate and water level are closer to the actual values, which shows that the simulation is accurate and reliable. Due to the sudden reduction of water cross section when the water flows through the weir and the strong change of water surface, the error of water level is larger than that of flow rate, but it is still close to the actual value.

Table 3: Simulated flow and water level errors

Design flow /(m <sup>3</sup> ·s <sup>-1</sup> )	Simulated flow /(m <sup>3</sup> ·s <sup>-1</sup> )	Flow relative error /%	Design depth /m	Simulated depth /m	Relative error of depth /%
0.11053	0.11071	0.16	0.40	0.42	5.00
0.10272	0.10292	0.19	0.37	0.39	5.41
0.09385	0.09402	0.18	0.35	0.38	8.57
0.08627	0.08657	0.35	0.34	0.36	5.88
0.07593	0.07609	0.21	0.32	0.34	6.25
0.06814	0.06828	0.21	0.29	0.30	3.45
Mean relative error		0.22	Mean relative error		5.76

### III. B. 2) Flow level relationship curves

The design flow level curve and the simulated flow level curve are plotted in the same coordinates, and the water level flow relationship curve is shown in Figure 5. It can be seen that the design flow water level curve and the simulated flow water level curve of the trend is basically the same, the trend line function are exponential function, and the two curves are basically close to each other, indicating that the two have a unified water level flow relationship.

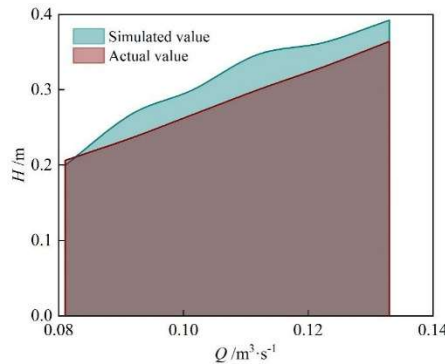


Figure 5: Relation curve of water level and discharge

### III. B. 3) Flow velocity distribution at different weir heights

Different weir heights were selected for simulation under the same water level and flow conditions to observe the effect of weir height on the flow velocity distribution. The effect of different weir heights on the flow velocity is shown in Fig. 6. Among them, (a)~(e) represent the distribution of flow velocity when the weir height is 0.12m, 0.18m, 0.24m, 0.30m and 0.36m under the flow rate of  $Q = 0.08527 \text{ m}^3 / \text{s}$ , respectively.

From Figure 6, we can see that the weir height has a great influence on the distribution of flow velocity, the larger the weir height, the more drastic the change of flow velocity, the change of flow velocity is mainly reflected in the weir after the section of the weir, the weir height of 0.12m, the weir before and after the flow velocity is small and remain stable. When the weir height is 0.18~0.30m, with the increase of weir height, the flow velocity after weir increases sharply. When the weir height is 0.36m, the flow velocity after the weir changes the most, and the influence

range also increases. Moreover, the flow velocity in the same section after the weir increases as the weir height increases.

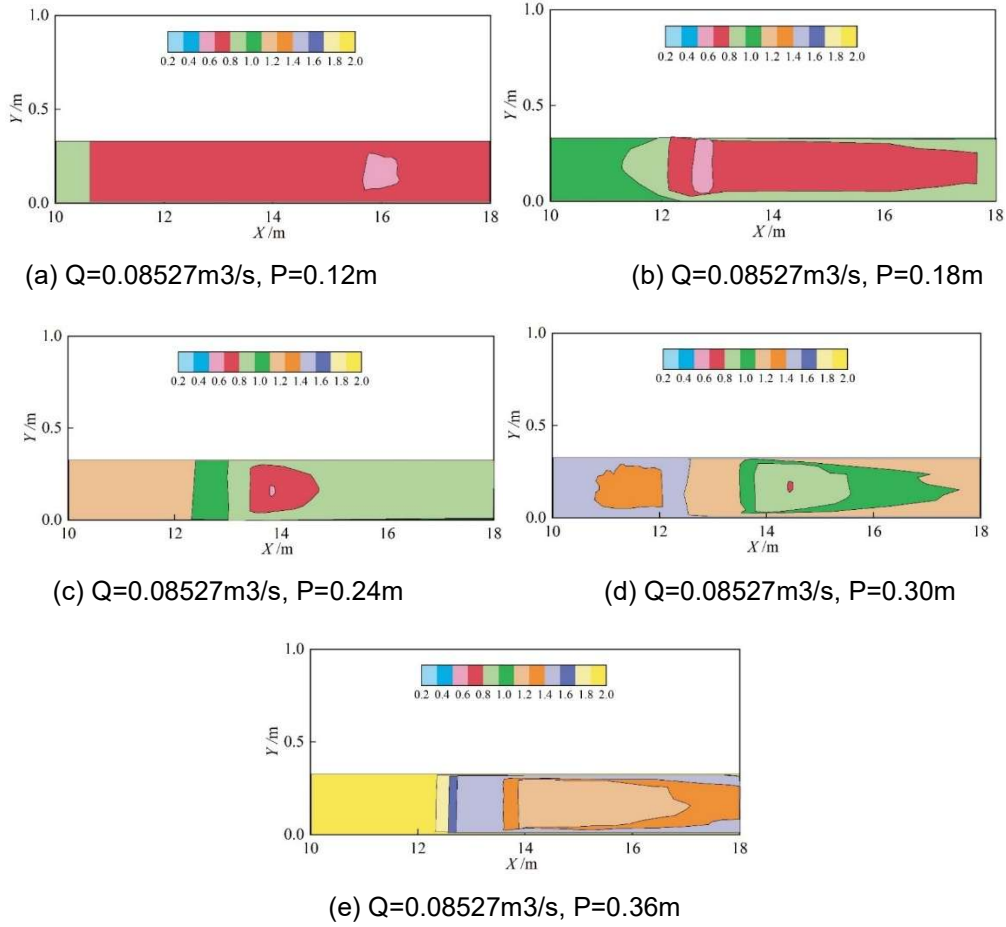


Figure 6: Velocity distribution of different weir heights

### III. C. Analysis of water level flow measurement sections in relation to flow rate

In this section, the improved long-throat channel gauging weir with a wide top weir is further structurally optimized to verify the superiority of the methodology in this paper. The research data mainly come from the measured data of the long-throat flume weir in the design and application project of river flow measurement and the simulation data in Winflume.

In Winflume, the geometric parameters of the long-throat channel gauging weir and the starting conditions of the water flow were defined, including the cross-sectional shape, length, slope, flow velocity, depth, and so on. Using Winflume software to carry out modeling and rate determination, establish the flow equation, flow table and flow curve in three forms of water level and flow relationship, to provide a strong basis for accurate water measurement.

According to the basic parameters of the No. 1 long-throat trough, using Winflume software for modeling and rate determination, the flow formula, flow table and flow curve in the form of three kinds of water level and flow relationship.

(1) Flow formula:

$$Q = 30.91(h_1 - 0.1)^{1.72} \quad (26)$$

where:  $Q$  that the flow,  $h_1$  that the radar water level meter measured upstream water level, the datum for the radar water level meter where the section of the channel bottom elevation.

Radar water level meter measured water level into this formula that can be known section flow.

(2) No. 1 long throat channel  $h_1 \sim Q$  curve shown in Figure 7.

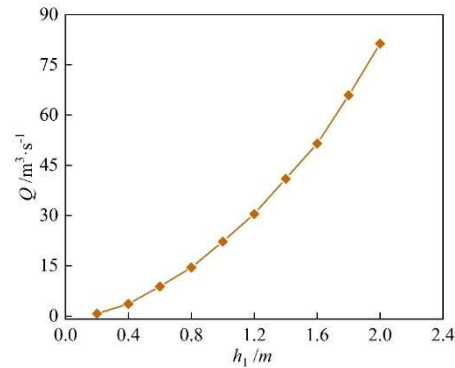


Figure 7: Number one long throat trough water level-flow curve

(3) The impact of the measurement deviation of the No. 1 water level gauge on the accuracy of flow measurement is analyzed as shown in Table 4.

These three forms of water level-flow relationship in the No. 1 long-throat trough set up in the canal section design flow rate  $Q = 31.82m^3/s$  range are applicable.

The measurement accuracy of radar water level meter is  $\pm 4mm$ , and the flow measurement accuracy of long throat trough within this deviation interval is analyzed. As can be seen from Table 4, the radar water level meter normal operation deviation range of long throat trough flow measurement accuracy control within 6%, in line with the flow measurement requirements of the water measuring trough. When the upstream water level is  $< 0.6m$ , the flow measurement accuracy of the long-throat trough is more sensitive to the deviation of water level measurement, and if it operates for a long period of time in this water level range, attention should be paid to regular calibration and maintenance of the radar water level meter to ensure the measurement accuracy. In view of the actual engineering applications, in the external environmental factors, the water surface at the station fluctuations, it is recommended to choose a more stable water flow time period of 3 ~ 5 times the average of the water level well measurements for the calculation, the use of the appropriate size of the connecting tube in the water level well has a better filtering effect.

Table 4: Analysis of flow measurement accuracy of number one long throat groove

Actual water level /m	Measuring water level /m		Measured flow / $(m^3.s^{-1})$		Actual flow / $(m^3.s^{-1})$	Accuracy of current measurement /%	
	$h_{1+4mm}$	$h_{1-4mm}$	$Q_{+4mm}$	$Q_{-4mm}$		+4mm	-4mm
0.200	0.204	0.196	0.729	0.664	0.702	3.846	-5.413
0.400	0.404	0.396	3.664	3.557	3.613	1.412	-1.550
0.600	0.604	0.596	8.905	8.721	8.824	0.918	-1.167
0.800	0.804	0.796	14.589	14.376	14.496	0.642	-0.828
1.000	1.004	0.996	22.293	22.085	22.190	0.464	-0.473
1.200	1.204	1.196	30.627	30.373	30.481	0.479	-0.354
1.400	1.404	1.396	41.174	40.816	40.968	0.503	-0.371
1.600	1.604	1.596	51.643	51.255	51.456	0.363	-0.391
1.800	1.804	1.796	66.171	65.672	65.878	0.445	-0.313
2.000	2.004	1.996	81.635	81.143	81.316	0.392	-0.213

## IV. Conclusion

In this paper, trapezoidal water measuring weir, triangular water measuring weir and long-throat trough water measuring weir are selected as the specific research objects, and the structural design of the weir and the optimization of the flow calculation method are realized based on the NLP method.

(1) By comparing the simulated head in front of the weir with the monitoring value of the new weir under different bottom hole heights and different flow conditions, it can be seen that the maximum relative error of the two results is 5.70%, and the simulation results are highly credible, which can ensure the accuracy. Considering the trapezoidal water measuring weir in the irrigation area, there is a small range of flow measurement and other problems, on the basis of the improved weir of  $b=280mm$ , the new weir is formed by adding an orifice with a height of 60 mm at the bottom, which has a wider range of flow measurement and good siltation prevention effect, and the maximum



relative error is 5.49%, which fully meets the requirements of the irrigation area for the accuracy of the water measurement.

(2) By comparing the simulated water level and flow rate relationship curve with the actual water level and flow rate relationship curve, it can be found that the curve has the same trend, are in line with the exponential function relationship, the two trend lines are relatively close to each other, and the two have a unified water level and flow rate relationship. The simulation of different weir heights under the same water level and flow conditions found that the weir height has a great influence on the flow rate distribution, and the larger the weir height is, the more drastic the change of flow rate is.

(3) Through the detailed analysis of the flow curve and flow table of the No.1 long-throat trough, the universality of the design flow range is verified, and the validity of the structural design optimization method of this paper is verified, and technical support is provided for the long-throat trough volume weir of the Shule River Basin.

## Funding

Leshan Science and Technology Planning Project (A312022019): Research on Design Method of Airfoil-shaped Measuring Flum with Shrinkage Ratio as index.

## References

- [1] Ma, T., Sun, S., Fu, G., Hall, J. W., Ni, Y., He, L., ... & Zhou, C. (2020). Pollution exacerbates China's water scarcity and its regional inequality. *Nature communications*, 11(1), 650.
- [2] Han, X., Zhao, Y., Gao, X., Jiang, S., Lin, L., & An, T. (2021). Virtual water output intensifies the water scarcity in Northwest China: Current situation, problem analysis and countermeasures. *Science of the Total Environment*, 765, 144276.
- [3] Huang, W., Shuai, C., Xiang, P., Chen, X., Zhao, B., & Sun, J. (2024). Assessing the consumption-based Water Use of Global Construction Sectors and its impact to the local water shortage. *Water Resources Management*, 1-16.
- [4] Liao, X., Zhao, X., Liu, W., Li, R., Wang, X., Wang, W., & Tillotson, M. R. (2020). Comparing water footprint and water scarcity footprint of energy demand in China's six megacities. *Applied Energy*, 269, 115137.
- [5] Zhou, K., Fan, Y., Gao, Z., Chen, H., & Kang, Y. (2024). Research progress on operation control and optimal scheduling of irrigation canal systems. *Irrigation and Drainage*.
- [6] Meng, X., & Wu, L. (2021). Prediction of per capita water consumption for 31 regions in China. *Environmental Science and Pollution Research*, 28, 29253-29264.
- [7] Wang, X., Xiao, X., Zou, Z., Dong, J., Qin, Y., Doughty, R. B., ... & Li, B. (2020). Gainers and losers of surface and terrestrial water resources in China during 1989–2016. *Nature communications*, 11(1), 3471.
- [8] Qin, J., Ding, Y. J., Zhao, Q. D., Wang, S. P., & Chang, Y. P. (2020). Assessments on surface water resources and their vulnerability and adaptability in China. *Advances in Climate Change Research*, 11(4), 381-391.
- [9] Zhao, Y., Wang, L., Jiang, Q., & Wang, Z. (2025). Spatiotemporal nonlinear characteristics and threshold effects of China's water resources. *Journal of Environmental Management*, 373, 123633.
- [10] Li, C., Jiang, T. T., Luan, X. B., Yin, Y. L., Wu, P. T., Wang, Y. B., & Sun, S. K. (2021). Determinants of agricultural water demand in China. *Journal of Cleaner Production*, 288, 125508.
- [11] Liu, P., Fang, Z., Lv, C., & Ruan, A. (2020). China's agricultural water-use efficiency and its influencing factors under the constraint of pollution emission. *International Journal of Design & Nature and Ecodynamics*, 15(4), 579-585.
- [12] Ju, Q., Du, L., Liu, C., & Jiang, S. (2023). Water resource management for irrigated agriculture in China: Problems and prospects. *Irrigation and Drainage*, 72(3), 854-863.
- [13] Wu, D., Cui, Y., Li, D., Chen, M., Ye, X., Fan, G., & Gong, L. (2021). Calculation framework for agricultural irrigation water consumption in multi-source irrigation systems. *Agricultural Water Management*, 244, 106603.
- [14] Sun, H., Wang, S., & Hao, X. (2017). An Improved Analytic Hierarchy Process Method for the evaluation of agricultural water management in irrigation districts of north China. *Agricultural Water Management*, 179, 324-337.
- [15] Liu, X., Yongde, K., Junning, L., & Zengxiang, J. (2024). Analysis and numerical simulation of different flowmeters based on an open channel in an irrigation area. *AQUA—Water Infrastructure, Ecosystems and Society*, 73(10), 2079-2092.
- [16] Howe, W. H., & Lipták, B. G. (2020). Weirs and Flumes. In *Flow Measurement* (pp. 192-196). CRC Press.
- [17] Gang, L. I. N. G., Wen, W. A. N. G., Hui, W. A. N. G., & Xiaotao, H. U. (2023). Numerical Study of Hydraulic Performance of Weir-flume Combined Device. *Journal of Irrigation & Drainage*, 42(10).
- [18] Tallat, R., & Chandra, N. (2024). Synthesis and Fabrication of High-Performance p-Type Silicon Nanowire Transistors[J], *TK Techforum Journal (ThyssenKrupp Techforum)*, 2024 (2). 32-39.
- [19] Fatxullojev, A., Gafarova, A., & Hamroqulov, J. (2021). Improvement of water accounting for irrigation systems. In *IOP Conference Series: Materials Science and Engineering* (Vol. 1030, No. 1, p. 012145). IOP Publishing.
- [20] Mohammadi, A., Rizi, A. P., & Abbasi, N. (2019). Field measurement and analysis of water losses at the main and tertiary levels of irrigation canals: Varamin Irrigation Scheme, Iran. *Global Ecology and Conservation*, 18, e00646.
- [21] Na Qin, Lei Liu, Lai Wei & Haibiao Chen. (2025). Exploring the development of electrocatalysts through an automated comprehensive literature review using NLP. *Journal of Alloys and Compounds Communications*, 6, 100067-100067.
- [22] R. de Vries, E.O.L. Lantsoght, R.D.J.M. Steenbergen, M.A.N. Hendriks & M. Naaktgeboren. (2025). Corrigendum to "Structural reliability updating on the basis of proof load testing and monitoring data" [Eng Struct 330 (2025) 119863]. *Engineering Structures*, 330, 119937-119937.
- [23] Connor, E. J. (2024). Evaluation of Bending Properties in Cold-Formed Stainless Steel Hollow Sections[J], *TK Techforum Journal (ThyssenKrupp Techforum)*, 2024 (2). 25-31.